INSAT geostationary meteorological satellite program and current meteorological data processing system for INSAT-3D/3DR/3DS at India Meteorological Department

R.K. Giri*, Satya Prakash, Ramashray Yadav, and K.C. Saikrishnan
*India Meteorological Department, MoES, Lodi Road, New Delhi.
Email: rk.giriccs@gmail.com

ABSTRACT

This paper reviews the Indian geostationary meteorological satellite program - INSAT, which started in 1982. Successive improvements in meteorological payloads onboard the INSAT-series satellites, and their spatial and temporal resolutions are also highlighted. Currently, third generation of INSAT satellites - INSAT-3D and INSAT-3DR are in orbit and providing huge volume of data from their meteorological payloads. Imager payloads of both satellites are kept in staggered mode to provide new dataset at 15-minutes interval. Sounder payload onboard the INSAT-3D is declared its end of life in September 2020, and currently INSAT-3DR sounder provides useful data at hourly interval. In order to complete processing of these enormous data from INSAT-3D and INSAT-3DR satellites and their timely dissemination to users, Multi-mission Meteorological Data Receiving and Processing System (MMDRPS) was installed at the India Meteorological Department (IMD), New Delhi. Different imageries and geophysical products generated from the imagers and sounder along with their potential applications are also briefly discussed.

Keywords: *Indian National Satellite (INSAT); Very High Resolution Radiometer (VHRR); Infrared Sounder; Charge Coupled Device (CCD); Indian Space Research Organisation (ISRO); Multi-mission Meteorological Data Receiving and Processing System (MMDRPS).*

1. An Overview of INSAT Meteorological Satellite Program

The Indian National Satellite (INSAT) program is a series of multipurpose Indian geostationary satellites intended to satisfy the telecommunication, broadcasting, meteorology, and search & rescue operations (Kelkar et al., 1992). The multipurpose concept of INSAT satellites led to the realization of full potential of geostationary satellites in a seamless manner. With the launch of the first satellite in the series of INSAT namely, INSAT-1A satellite on 10th April, 1982, satellite meteorology accelerated tremendously in India. The INSAT meteorological satellite system has an exceptional evolution since 1982 (Table 1). Currently, India has third generation of INSAT satellites in orbit. The first four satellites in the INSAT-1 series were only designed by India but fabricated in the U.S. and launched by foreign rockets. However, INSAT-2 series of satellites and INSAT-3A/3D were designed as well as fabricated indigenously by the Indian Space Research Organisation (ISRO). The latest satellite of the INSAT series namely, INSAT-3DR was completely made (both designed and fabricated) in India and also launched from India with an Indian geostationary satellite launch vehicle. A comprehensive review of the INSAT meteorological satellite program is given by Joshi et al. (2003), Kelkar (2019), and Bhatia and Mitra (2021).

While INSAT-1 series satellites consisted of multipurpose payloads, some of the later satellites have not any meteorological instrument. On the other hand, METSAT, launched in 2002 and later renamed as Kalpana-1, was the first exclusive meteorological satellite in the INSAT series (Kaila et al., 2002). INSAT-3D is the first Indian geostationary satellite to carry a sounder. It is primarily a meteorological satellite and has no communication transponder except for Data Relay Transponder (DRT) and Satellite-Aided Search & Rescue (SAS&R) payloads. DRT payload is used for receiving meteorological, hydrological and oceanographic data from remote, uninhabited locations over the satellite coverage area from the data collection platforms such as automatic weather

Table 1. A brief description of INSAT series geostationary meteorological satellites.

Satellite	Launch	Position	Met. Payloads	VHRR/CCD Channels	Spatial Resolution	Temporal Resolution
INSAT-1A INSAT-1B INSAT-1C INSAT-1D	Apr 1982 Aug 1983 Jul 1988 Jun 1990	74ºE 74ºE 93.5ºE 83ºE	VHRR	Vis (0.55-0.75 µm) TIR (10.5-12.5 µm)	2.75 km 11 km	3-hourly
INSAT-2A INSAT-2B	Jul 1992 Jul 1993	74ºE 93.5ºE	VHRR	Vis (0.55-0.75 µm) TIR (10.5-12.5 µm)	2 km 8 km	3-hourly
INSAT-2E	Apr 1999	83ºE	VHRR	Vis (0.55-0.75 µm) WV (5.7-7.1 µm) TIR (10.5-12.5 µm)	2 km 8 km 8 km	3-hourly
			CCD	Vis (0.62-0.68 µm) NIR (0.77-0.86 µm) SWIR (1.55-1.69µm)	1 km	Six times daily (03,05,06,07,09 & 11 UTC)
Kalpana-1 (MetSat-1)	Sep 2002	74ºE	VHRR	Vis (0.55-0.75 µm) WV (5.7-7.1 µm) TIR (10.5-12.5 µm)	2 km 8 km 8 km	3-hourly (2002 – 2005) Hourly (2005 – 2008) Half-hourly (2008-2017)
INSAT-3A	Apr 2003	93.5ºE	VHRR	Vis (0.55-0.75 µm) WV (5.7-7.1 µm) TIR (10.5-12.5 µm)	2 km 8 km 8 km	3-hourly (2003 – 2008) Hourly (2008 – 2016)
			CCD	Vis (0.62-0.68 µm) NIR (0.77-0.86 µm) SWIR (1.55-1.69 µm)	1 km	Six times daily (03,05,06,07,09 & 11 UTC)
INSAT-3D INSAT-3DR	Jul 2013 Sep 2016	82ºE 74ºE	VHRR Sounder	Vis (0.55-0.75 µm) SWIR (1.55-1.70 µm) MIR (3.80-4.00 µm) WV (6.5-7.1 µm) TIR1 (10.3-11.3 µm) TIR2 (11.5-12.5 µm)	1 km 1 km 4 km 8 km 4km 4 km	Half-hourly

stations, automatic rain gauges and Agromet stations. All INSAT-series meteorological satellites listed in Table 1 had a DRT payload onboard. SAS&R payload started from INSAT-2 series satellites, and it is not a meteorological instrument. It is used to pick up and relay alert signals originating from the distress beacons of maritime, aviation and land-based users to the Indian Mission Control Centre.

The capability of the imaging radiometers namely, Very High Resolution Radiometer (VHRR) carried by the INSAT satellites has increased successively. INSAT-1 series satellites viz., INSAT-1A/B/C/D and INSAT-2A/B carried a 2-channel VHRR operating in visible (0.55-0.75 µm) and thermal infrared (TIR; 10.5-12.5 µm) regions (Joseph et al., 1994). Their resolutions at the sub-satellite point were 2.75 km for visible channel and 11 km for TIR channel in case of INSAT-1 series satellites, which increased to 2 km for visible and 8 km for TIR in case of INSAT-2 series satellites and INSAT-3A satellite. The INSAT-2E satellite, for the first time carried a 3-channel VHRR with an additional water vapour channel (WV; 5.7-7.1 µm) having spatial resolution of 8 km (Bhatia et al., 1999). This satellite also carried the first Charge-Coupled Device (CCD) instrument having three channels in visible (0.62-0.68 µm), near infrared (NIR; 0.77-0.86 µm) and shortwave infrared (SWIR; 1.55-1.69 µm) regions (Bhatia and Gupta, 1999). CCD instrument provided day-time imaging at a spatial resolution of 1 km for each channel. The design of the VHRR systems on the INSAT-3A and Kalpana-1 was similar to that of INSAT-2E. Similar to INSAT-2E, INSAT-3A also carried CCD payload for day-time imaging. The temporal resolution of the VHRR payload is also increased from 3-hourly in the INSAT-1/2 series to half-hourly in Kalpana-1 and INSAT-3A from 2008 and INSAT-3D/3DR satellites. Both INSAT-3A and Kalpana-1 had been decommissioned and discontinued since September

2016 and September 2017, respectively. Meteorological observations and derived products from these INSAT series satellites have shown to be vital for a wide range of applications including weather monitoring and prediction (Veeraraghavan and Tiwari, 1984; Pal et al., 1989; Kelkar and Rao, 1990; Agnihotri, 1993; Singh et al., 2006; Singh et al., 2007; Srinivasan and Joshi, 2007; Bhatia and Sharma, 2013; Bhattacharya et al., 2013; Konduru et al., 2013; Manikiam and Nagaraja, 2015; Patel et al., 2015; Vyas et al., 2015; Chattopadhyay et al., 2016; Kishtawal, 2016, 2019; Agarwal et al., 2019; Nayak, 2020; Vyas and Bhattacharya, 2020).

2. INSAT-3D & 3DR satellites

At present, two operational meteorological satellites in the INSAT-series namely, INSAT-3D and INSAT-3DR are in orbit. INSAT-3D, launched on 26th July, 2013, is the most advanced Indian meteorological satellite located at 82ºE (Katti et al., 2006). It has a 6-channel imager and a 19-channel atmospheric sounder. The INSAT-3D imager is an improved design of the VHRR instrument flown on the Kalpana-1 and INSAT-3A missions. It is capable of generating the images of the Earth in six wavelength bands namely, visible (0.55-0.75 μm), shortwave infrared (SWIR; 1.55-1.70 μm) of spatial resolution 1 km, mid infrared (MIR; 3.80-4.00 μm), thermal infrared-1 (TIR1; 10.30-11.30 μm), thermal infrared-2 (TIR2; 11.50-12.50 μm) of spatial resolution 4 km and water vapour (WV; 6.50-7.10 μm) of spatial resolution 8 km. The selection of these six channels is based on their distinct weighting functions and applicability. Visible and SWIR channels are based on reflectance of the electromagnetic radiation, weighting functions of emission based MIR, WV, TIR1 and TIR2 channels are shown in Figure 1. TIR channel was first time split into two channels - TIR1 and TIR2 in INSAT-3D VHRR for more accurate sea surface temperature (SST) estimation. TIR2 is about two times more sensitive to low-level WV than TIR1, and is also called the dirty window channel. The difference between TIR1 and TIR2 measurements quantifies the differential WV absorption in the atmosphere and used to correct the atmospheric absorption of the upwelling radiation to obtain more accurate SST estimate (Mathur et al., 2006; Jangid

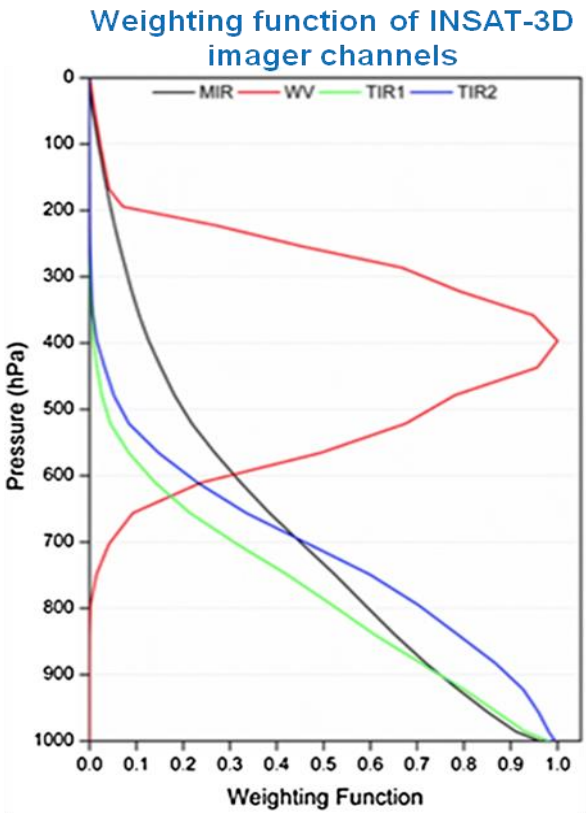

Figure 1: Weighting functions of INSAT-3D/3DR VHRR channels (Rani et al., 2019).

et al., 2017; Ojha and Singh, 2019; Gangwar and Thapliyal, 2020). MIR channel was introduced to provide night-time fog and low cloud detection. In addition, MIR along with SWIR channel enables better land-cloud discrimination and detection of surface features. The assimilation of clear-sky WV brightness temperature from the INSAT-3D VHRR in the National Centre for Medium Range Weather Forecasting (NCMRWF) Unified Model (NCUM) showed positive impact on humidity and upper tropospheric wind field forecasts. Consequently, it is operationally assimilated in the NCUM since 2018 (Rani et al., 2019). Moreover, the assimilation of all-sky WV channel imager radiance demonstrated positive impact than clear-sky WV radiances in short-range weather forecasts (Kumar et al., 2022).

INSAT-3D also carries a 19-channel sounder, which is the first such payload onboard an Indian satellite mission. The sounder consisting of 7 channels of longwave infrared (LWIR; 14.71-12.02 μm), 5 channels of midwave infrared (MWIR; 11.03-6.51 μm), 6 channels of SWIR (4.572-3.74 μm) and one channel of visible (0.695 μm) scans

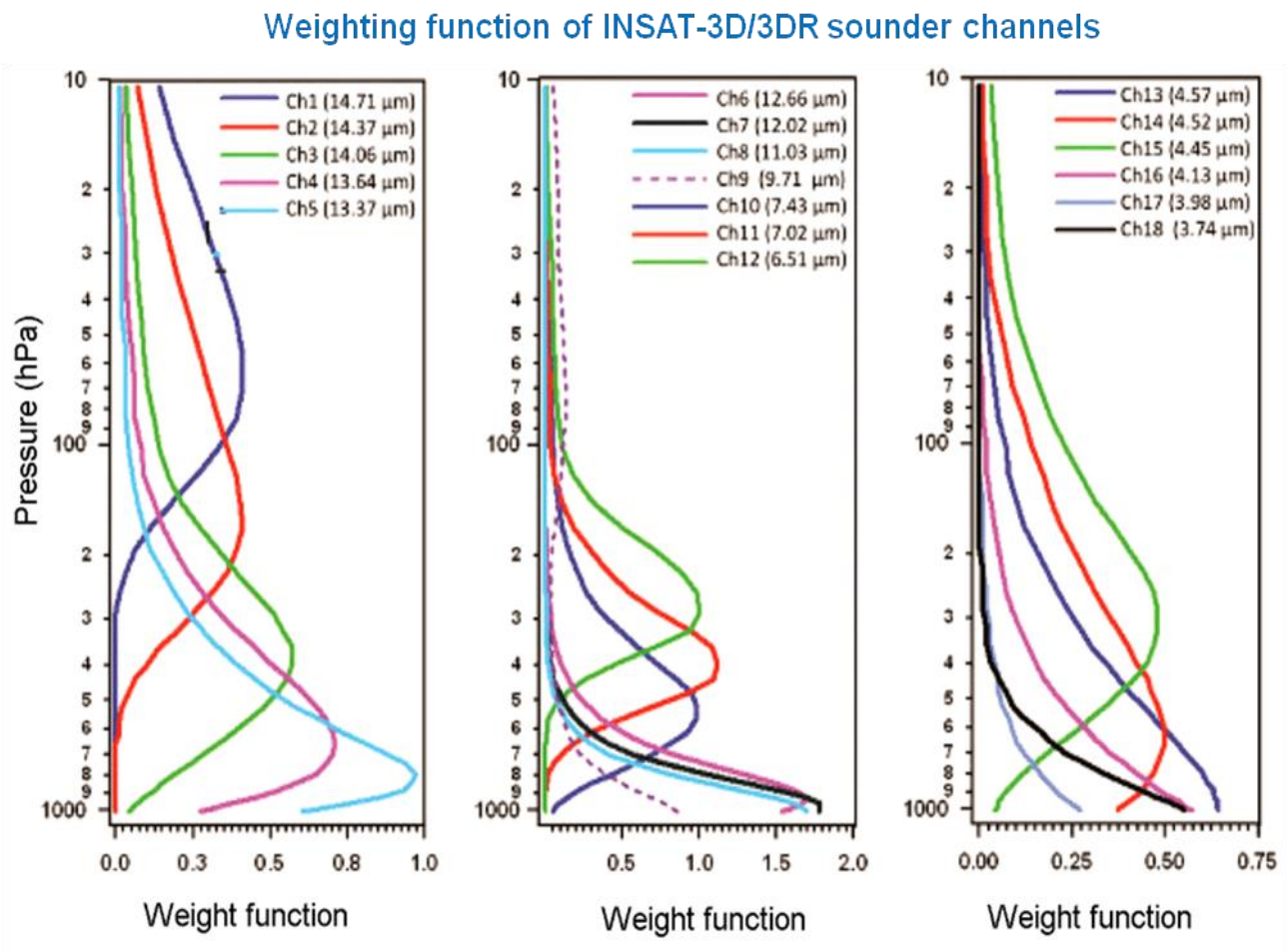

Figure 2: Weighting functions of INSAT-3D/3DR sounder channels (Kishtawal, 2019).

the atmosphere for derivation of profiles. The ground resolution at nadir is nominally 10 km × 10 km for all 19 channels of the sounder. The weighting functions of each channel of the sounder except for the visible channel for a monsoon month are shown in Figure 2. A numerical experiment of assimilation of clear-sky radiances from INSAT-3D VHRR WV, TIR1 and TIR2 channels and 18 IR channels of sounder showed significant improvement in short-term forecasts of moisture, temperature, precipitation and wind fields. However, the assimilation of sounder radiances showed larger impact than VHRR radiances (Singh et al., 2016a). The improved tropical cyclone prediction over the Bay of Bengal through the assimilation of sounder radiance data in a numerical model was also demonstrated by Nadimpalli et al. (2020).

INSAT-3DR was launched on 08th September, 2016 and located at 74^{o}E, which serves as a full on-orbit backup for INSAT-3D. INSAT-3DR carries similar payloads to INSAT-3D. Both VHRRs onboard INSAT-3D and INSAT-3DR have temporal resolutions of 30-minutes. Therefore, 48 full disc images are acquired daily from each INSAT-3D and INSAT-3DR imager payloads. However, both VHRRs are used in stagger mode so that after every fifteen minutes, a new set of images/product become available to the users. The VHRR onboard INSAT-3DR has an additional capability of rapid-scan, which is turned on during the formation of tropical cyclones over the North Indian Ocean (Mohapatra et al., 2021). During the rapid-scan period, the VHRR provides data for specific six blocks (out of 36 blocks of full disc image) at about 4.5-minutes interval. Figure 3 shows an example of rapid-scan images within 30-minutes from the INSAT-3DR imager and the corresponding full disc image from the INSAT-3D imager during a tropical cyclone in the Bay of Bengal. It can be seen that rapid-scan facility provides six images of the tropical cyclone within half an hour, whereas users get one full disc image in this period under normal

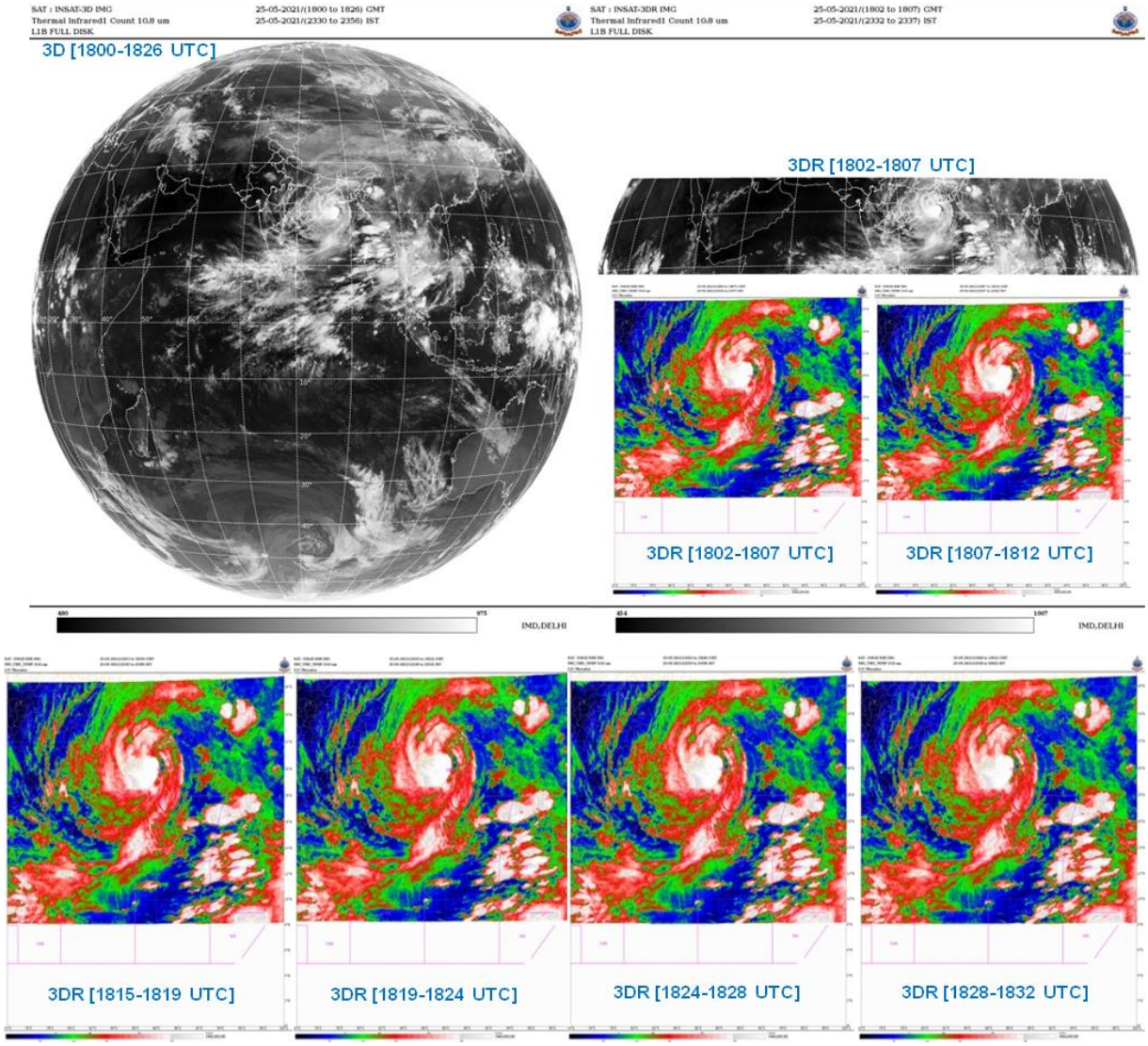

Figure 3: An illustration of rapid-scan images from the INSAT-3DR during the Yaas cyclone on 25 May, 2021. The corresponding INSAT-3D full disc image is also shown.

operation of the VHRR. Rapid-scan images are very important to characterize and study the rapid changes in the severe weather systems such as tropical cyclones (Ahmed et al., 2022; Jaiswal et al., 2022).

The INSAT-3D sounder has been declared its end of life in September 2020, and only INSAT-3DR is now providing useful sounder data. The temporal resolution of sounder is one hour. The scanning mechanism of sounder is completely different than the VHRR and it was revised for INSAT-3DR in October 2020 after decommissioning of INSAT-3D sounder. The current scanning mechanism of INSAT-3DR sounder is shown in Figure 4. The sounder provides data for either sector A covering Indian landmass or sector B covering Indian Ocean region. At present, INSAT-3DR sounder provides four images for Sector B and twenty images for Sector A daily. The qualitative products generated after processing these satellite data (both imager and sounder) are disseminated to users for use in weather forecasting and other applications. In addition to VHRR and sounder, both satellites have DRT payloads to receive and transmit in-situ data from automatic weather stations, automatic rain gauge and agromet station network of different institutions from all over India. Also, both satellites have SAS&R instruments onboard. Similar to INSAT-3D and INSAT-3DR satellites, INSAT-3DS satellite is planned to be launched this year in 2023. INSAT-3DS will also have similar meteorological payloads, viz. six-channel VHRR and 19-channel atmospheric sounder.

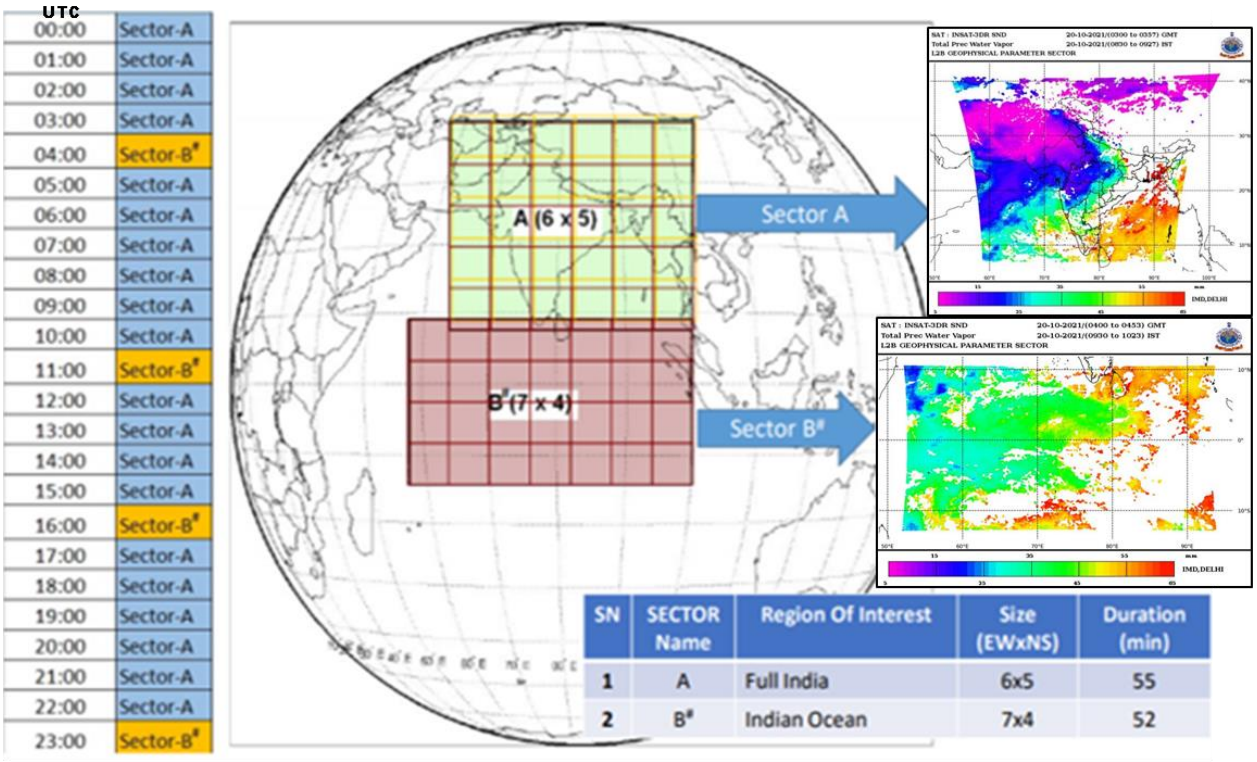

SN	SECTOR Name	Region Of Interest	Size (EWxNS)	Duration (min)
1	A	Full India	6x5	55
2	B#	Indian Ocean	7x4	52

Figure 4: INSAT-3DR sounder scan sectors and corresponding scan times. Total precipitable water products for both sectors (i.e., sectors A and B) for a typical day are also shown.

3. MMDRPS at IMD, New Delhi

The Multi-mission Meteorological Data Receiving and Processing System (MMDRPS) is a state-of-the-art very advanced meteorological data processing system. This system is established at National Satellite Meteorological Centre of the India Meteorological Department (IMD), New Delhi in collaboration with ISRO. This system is operational in IMD since 2020, and has been formally inaugurated by the Honorable Union Minister of Science and Technology and Earth Sciences, Government of India on 15 January, 2021. The MMDRPS is an end-to-end real-time data processing system with three dedicated Earth station antennas that enables acquisition, processing, archival, and dissemination of complete meteorological data from the VHRR, sounder and DRT payloads of the INSAT-3D, INSAT-3DR and upcoming INSAT-3DS satellites (Figure 5). The system consists of about 100 servers and workstations, and two-tier objective type storage of capacity 2 PB each with 324 TB solid state drive system. This system is very fast as compared to the previous INSAT Meteorological Data Processing System (IMDPS), and consequently data reception to product generation time is now reduced from 20 minutes for IMDPS to 7 minutes for MMDRPS. The MMDRPS is also capable to process rapid-scan data of INSAT-3DR imager conducted during tropical cyclones over the North Indian Ocean in real-time. The MMDRPS outputs are widely utilized for monitoring of severe weather and many sectorial applications such as defense services, disaster management, power sector, aviation, railway, tourism and agriculture. The MMDRPS products are available on the dedicated webpages at http://satellite.imd.gov.in/ and https://satmet.imd.gov. in , and geo-referenced satellite data can be visualized and analyzed through the online visualization tool known as Real-time Analysis of Products & Information Dissemination (RAPID; https://rapid.imd.gov.in/r2v/). RAPID is an interactive web-based tool to visualize and analyze the INSAT-3D/3DR satellite data (also radar, ground observations and NWP model outputs) in real-time and provides features of interest to the scientific community.

Data products generated from INSAT-3D and INSAT-3DR VHRRs and INSAT-3DR sounder through the MMDRPS are briefly described here.

Figure 5: High-end servers and antenna of the MMDRPS at IMD, New Delhi.

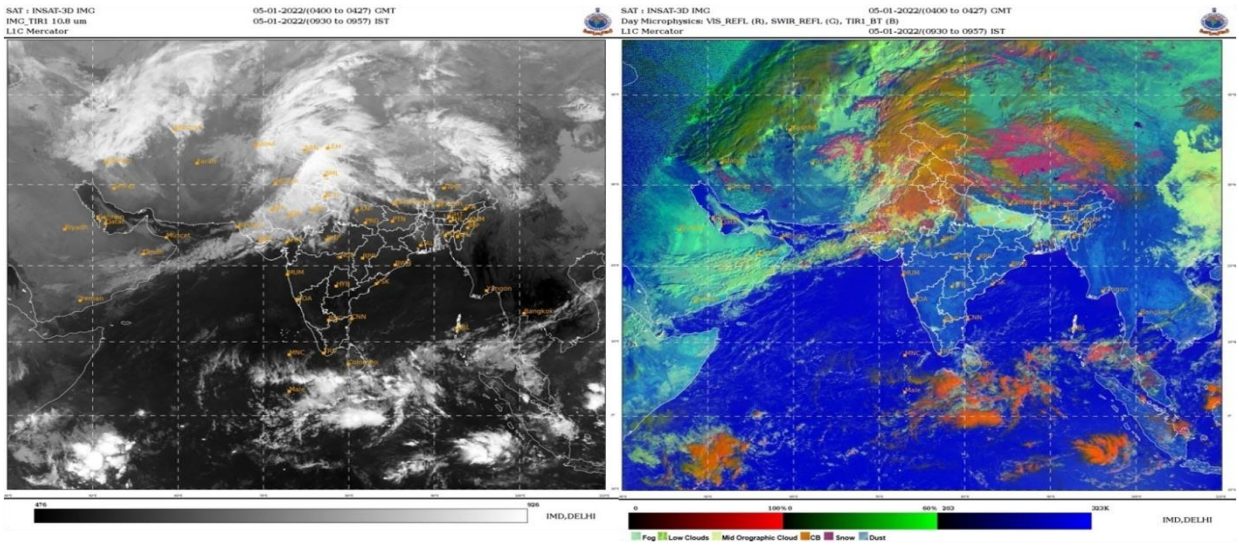

Figure 6: An illustration of western disturbance (WD) over the northern & western India and fog over the Himalayan foothills (e.g., east Uttar Pradesh, Bihar, North West Bengal and Bangladesh) in the INSAT-3D TIR1 image and corresponding RGB image during 5 January, 2022.

3.1 Data Products from INSAT-3D and INSAT-3DR Imager or VHRR

INSAT-3D and INSAT-3DR VHRR imageries for six channels viz. visible, SWIR, MIR, WV, TIR1, and TIR2 along with brightness temperatures at MIR, WV, IR1 and IR2 channels and day/night microphysics are generated half-hourly for the full disc and for several sectors such as (a) Asia sector, (b) High resolution Asia sector, (c) Northeast sector, (d) Northwest sector, (e) Southeast sector or Bay of Bengal, (f) Southwest sector or Arabian Sea, (g) Aviation sector, (h) Aviation sector with routes, and (i) Pilgrimage sector. These imageries are also generated operationally for other South Asian Association for Regional Cooperation (SAARC) countries namely, Afghanistan, Bangladesh, Bhutan, Maldives, Nepal, Pakistan and Sri Lanka. A complete list of VHRR imageries and products generated through the MMDRPS operationally with the help of Space Applications Centre (SAC)-ISRO is given in Table 2.

Day microphysics or RGB product uses visible reflectivity, SWIR reflectivity and TIR1 brightness temperature, while night microphysics uses MIR brightness temperature, TIR1 brightness temperature and TIR2 brightness temperature. These RGB products are shown to be very useful for the identification and monitoring of severe weather events (Mitra et al., 2018a, 2019). Figure 6 shows an example of clouds associated with Western Disturbance (WD) and fog or low clouds over the western and northern parts of India. The

identification and discrimination of WD clouds and fog in TIR1 image are rather difficult, whereas they can easily be distinguished in the corresponding RGB image. This example demonstrates the advantage of RGB imagery over a single channel VHRR imagery for identification and monitoring of weather systems. In addition, two cyclone enhancement images such as the Dvorak enhancement curve or BD Curve and IMD Curve (analogous to National Hurricane Center (NHC) Curve) are also generated regularly. These imageries play vital role in the estimation of centre, cloud pattern, and intensity of the tropical cyclones especially over the open ocean through the Dvorak technique (Dvorak, 1975; Velden et al., 2006; Goyal et al., 2017a; Ahmed et al., 2021). During the cyclonic conditions over the North Indian Ocean, INSAT-3DR operates in the rapid-scan mode and provides images at about 4.5-minutes interval.

INSAT imageries are basically used in three ways: (i) to monitor in-situ growth of weather phenomena like cumulonimbus clouds, fog, etc., (ii) to monitor the movement of migratory systems like tropical cyclones, western disturbances or monsoon depressions and (iii) to identify or locate primary synoptic elements such as surface lows, troughs and ridges, jet streams and regions of intense convection. There are several geophysical products operationally derived from the INSAT-3D/3DR VHRR measurements. Higher temporal resolution and finer spatial resolution of these geophysical products make them vital for the study of dynamic atmospheric and oceanic features (Agarwal et al., 2019; Mohapatra et al., 2021). A complete list of these products is given in Table 2 and few major products are briefly described below. Details of the algorithms utilized for development of these geophysical products are given by SAC (2015). Some of the VHRR products are gridded products, whereas some of them are pixel level and point level products.

3.1.1 Outgoing Longwave Radiation (OLR)

The total amount of the thermal radiation that is emitted from the Earth-atmosphere system to the outer space is called Outgoing Longwave Radiation (OLR). OLR is strongly controlled by three main meteorological variables, namely the temperature of the Earth and the atmosphere above it, the presence of water vapour in the atmosphere, and the presence of clouds. The OLR estimates are useful for various applications in climate sensitivity and diagnostics, numerical weather forecasting and climate models. Generally, OLR values less than 250 Wm^{-2} would give a good indication of the cloudiness over the tropics (Ghanekar et al., 2010). WV, TIR1 and TIR2 channels of VHRRs are used as input for the development of OLR product (Singh et al., 2007). This product is generated half-hourly from both INSAT-3D and 3DR satellites for 50ºS-50ºN and 35ºE-135ºE at pixel scale (~4 km). Recently, daily gridded OLR product from INSAT-3D was prepared for 2014-2020 at 10 km resolution and found to be reasonable as compared to the Clouds and Earth's Radiant Energy System (Yadav et al., 2022).

3.1.2 Sea Surface Temperature (SST)

Sea surface temperature (SST) is among the essential climate variables, and plays vital role in the air-sea interactions, oceanic circulation and global water cycle. Accurate estimates of SST are crucial for the global climate change assessment and numerical weather and climate prediction models. SST estimates from both INSAT-3D and INSAT-3DR satellites are derived from split thermal window channels (TIR1 and TIR2) during day-time and using additional MIR window channel during night-time over cloud-free oceanic regions (Ojha and Singh, 2019; Gangwar and Thapliyal, 2020). Although infrared-based SST estimates are available at finer spatial resolution, the presence of atmospheric water vapour, clouds and aerosols limits their consistent availability. This product is generated half-hourly from both INSAT-3D and INSAT-3DR satellites for 40ºS-40ºN and 30ºE-120ºE at pixel scale (~4 km).

3.1.3 Land Surface Temperature (LST)

Land surface temperature (LST) is one of the key parameters for the land surface process and climate studies at global and regional scales. It is one of the crucial inputs to weather and climate prediction models, climate change detection, vegetation health

Table 2. List of INSAT-3D/3DR Imager products operationally generated through the MMDRPS at IMD, New Delhi

INSAT-3D/3DR Imager Products	
Full Disk (11 images)	Vis, WV, SWIR, MIR, IR1, IR2, MIR-Brightness Temperature (BT), WV-BT, IR1-BT, IR2-BT, Day/Night Microphysics
Asia Sector (14 images)	Vis, WV, SWIR, MIR, IR1, IR2, MIR-BT, WV-BT, IR1-BT, IR2-BT, Day/Night Microphysics, IR1-Blended, CTBT, VIS+IR1BT sandwich
Asia Sector High Resolution (13 images)	Vis, WV, SWIR, MIR, IR1, IR2, MIR-BT, WV-BT, IR1-BT, IR2-BT, Day/Night Microphysics, BD Curve, NHC Curve
NE Sector (8 images)	Vis, SWIR, MIR, IR1, MIR-BT, IR1-TB, Day/Night Microphysics, RGB
NW Sector (8 images)	Vis, SWIR, MIR, IR1, MIR-BT, IR1-TB, Day/Night Microphysics, RGB
Bay of Bengal or SE Sector (13 images)	Vis, WV, SWIR, MIR, IR1, IR2, MIR-BT, WV-BT, IR1-BT, IR2-BT, Day/Night Microphysics, BD Curve, NHC Curve
Arabian Sea or SW Sector (13 images)	Vis, WV, SWIR, MIR, IR1, IR2, MIR-BT, WV-BT, IR1-BT, IR2-BT, Day/Night Microphysics, BD Curve, NHC Curve
Aviation Sector (8 images)	IR1, Vis, SWIR, Cold Clouds, IR1 with route, Vis with route, SWIR with route, Cold Clouds with route
Pilgrimage (4 images)	IR1, Vis, SWIR, IR1-BT
SAARC (84 images)	IR1, MIR, WV, VIS, SWIR, IR1-BT, MIR-BT, WV-BT, Day/Night Microphysics, IR1-Blended, VIS+IR1 BT sandwich, CTBT
Geophysical Products (35 images)	Cloud Mask, Outgoing longwave radiation (OLR), Cloud top temperature (CTT), Cloud top pressure (CTP), Upper tropospheric humidity (UTH), Sea surface temperature (SST), Land surface temperature (LST), Total precipitable water (TPW), GOES Precipitation Index (GPI), IMSRA (IMR), Improved IMSRA (IMC), Hydro-estimator (HEM), Storm Index, Aerosol optical depth, Fog, Fog Intensity, Fire, Smoke, Snow, Surface insolation, Land surface albedo (LSA), Net effective radiation, Cloud particle effective radius (CER) , Cloud optical thickness (COT), Global horizontal irradiance (GHI), Diffused normal irradiance (DNI), Direct horizontal irradiance (DHI), Fractional clear area for MIR, WV, TIR1 & TIR2, Clear sky BT for MIR, WV, TIR1 & TIR2
Wind Derived Products (9 images)	Vorticity @850, 750, 500 & 200 hPa, Wind Shear, Shear Tendency, Mid Shear, Lower Convergence, Upper Divergence
Atmospheric Motion Vector (6 images)	IRW, MRW, WVW, VSW, HIGH, LOW
Binned 3-hourly (3 images)	IMR, IMC, HEM
Binned Daily (21 images)	MIR-BT, WV-BT, IR1-BT, IR2-BT, OLR, SST, LST Max, LST Min, UTH, GPI, IMR, IMC, HEM, Potential evapotranspiration, Actual evapotranspiration, Shortwave radiation over ocean, Surface insolation, LSA, DHI, DNI, GHI
Some geophysical products are also generated as 5-days, 7-days, 10-days, 15-days, and monthly composites.	

monitoring, drought, hydrological studies, forest fires, etc. LST estimates from both INSAT-3D and INSAT-3DR satellites are derived from split thermal window channels (TIR1 and TIR2) over cloud-free land regions (Pandya et al., 2011). This product is generated half-hourly from both INSAT-3D and INSAT-3DR satellites for 40ºS-40ºN and 50ºE-130ºE at pixel scale (~4 km). The assimilation of INSAT-3D derived LST in an NWP model demonstrated reduction in temperature and moisture forecast errors by 8-10% (Singh et al., 2016b). In addition, the assimilation of INSAT-3D LST observations in the NCUM global model showed a notable improvement in maximum and minimum temperature forecasts over India (Lodh et al., 2019).

3.1.4 Upper Tropospheric Humidity (UTH)

Upper Tropospheric Humidity (UTH) is an estimate of the mean relative humidity of the atmosphere approximately between 600 hPa and 300 hPa. UTH is basically a measure of weighted mean of relative humidity according to the weighting function of the WV channel. Therefore, UTH is more likely a representative of the relative humidity around the atmospheric layer where weighting function of WV channel peaks. UTH from satellite measurements is useful to monitor changes in WV in the upper troposphere. TIR1 and WV channels are used as input to derive the UTH product (Thapliyal et al., 2011). This product is generated half-hourly from both INSAT-3D and INSAT-3DR satellites for 50ºS-50ºN and 30ºE-130ºE at pixel scale (~4 km).

3.1.5 Quantitative Precipitation Estimate (QPE)

The quantitative assessment of precipitation is needed to improve understanding of the behavior of global energy and circulation patterns as well as the nature of climate variability. Precipitation is one of the most variable quantities in both space and time. Precipitation has direct impact on human life that other atmospheric phenomena seldom have. Geostationary weather satellites provide the rapid temporal update cycle needed to capture the growth and decay of precipitating clouds. The inherent limitations of optical channels remain persistent for rainfall retrieval as surface rainfall is inferred by cloud top signatures only. There is no direct physical connection between the rain/cloud and ice hydrometeors within the clouds with radiance emanating from cloud tops to the sensor. However, large spatial coverage and frequent observations of the geostationary optical measurements are very strong points along with the resolution capabilities of the sensors to retrieve rainfall.

Four QPE products namely, GOES Precipitation Index (GPI; Prakash et al., 2011; Gairola et al., 2014), INSAT Multispectral Rainfall Algorithm (IMR; Prakash et al., 2010; Gairola et al., 2014), Corrected IMR (IMC; Mahesh et al., 2014), and Hydro-Estimator Method (HEM; Varma and Sharma, 2022) are generated each half-hourly from both INSAT-3D and INSAT-3DR satellites. The spatial resolutions are 1º for GPI, 0.1º for IMR, and pixel-level (~4 km) for IMC and HEM products. HEM product requires additional NWP outputs such as total precipitable water, relative humidity, and zonal & meridional wind components from the National Centers for Environmental Prediction (NCEP) Global Forecasting System (GFS) model for the generation of QPE (Varma and Sharma, 2022). INSAT-3D derived IMR and HEM products showed positive impact on short-range rainfall prediction when assimilated in a NWP model (Kumar and Varma, 2017; Bushair et al., 2019). GPI product is reasonable for large-scale rainfall estimation at longer temporal scale. IMC product showed improvement over the IMR product for the southwest monsoon rainfall estimation (Khan et al., 2021; Prakash and Bhan, 2023b), whereas no improvement over IMR was evident for the tropical cyclone rainfall estimation (Prakash and Bhan, 2023a). IMR and IMC products were shown to be better for moderate monsoon rainfall estimation, while HEM was superior for heavy to very heavy rainfall estimation over the Indian region (Singh et al., 2018; Mitra et al., 2018b; Kumar et al., 2021; Malhan et al., 2022). IMR, IMC and HEM products are operationally generated at half-hourly, three-hourly and daily temporal scales.

3.1.6 Fog cover and Intensity

During winter months, the spread of fog in India is very large and it severely affects many activities such as road transport, railways and aviation sectors. Fog can reduce visibility to less than 1 km.

Thus, the spatial and temporal detection of fog becomes very important. The spatial and temporal resolutions of the geostationary satellites are beneficial for real-time detection of fog over large areas. Fog is a low-lying cloud and its spectral properties are more related to the underlying surface in comparison to middle and high level clouds. Fog products are generated throughout the day using spectral data of visible, MIR and TIR channels (Chaurasia and Gohil, 2015). For the detection of night-time fog, the brightness temperature difference (BTD) technique utilizing MIR and TIR channels is used and day-time fog is detected using temporal differencing technique utilizing visible and TIR1 data of INSAT-3D/3DR (SAC, 2015; Chaurasia and Jenamani, 2017). Detection of fog is represented in binary form such that value 1 indicates presence of fog and value 0 indicates no fog condition at pixel scale.

Fog is routinely detected from INSAT-3D and INSAT-3DR VHRRs and are classified into four categories according to its intensity. Based on visibility the categories are: 1) Shallow fog (500m >= visibility < 1000m), 2) Moderate fog (200m >= visibility < 500m), 3) Dense fog (50m >= visibility < 200m) and 4) Very dense fog (visibility < 50m). Based on the corresponding BTD values during night-time and change in reflectance value during the day-time, fog intensity product is generated at pixel scale.

3.1.7 Atmospheric Wind Products

Six products namely, cloud motion vector wind derived from TIR1 channel, MIR wind derived from MIR channel, WV wind derived from WV channel, visible wind derived from visible channel, high level wind derived from TIR1 and WV channels, and low level wind derived from TIR1, MIR and visible channels are regularly generated through the MMDRPS (Deb et al., 2018, 2020; Sankhala et al., 2019). These are point level products. There are four basic steps involved in atmospheric wind products or atmospheric motion vectors (AMVs) generation: (a) Tracer selection, (b) Height assignment, (c) Tracking and (d) Wind buffer generation and quality control. NWP outputs along with VHRRs measurements are also utilized in generation of these products. AMVs from the INSAT-3D satellite were found to be comparable with Meteosat-7 derived AMVs over the Indian Ocean and assimilation of INSAT-3D/3DR AMVs through NWP models improved the simulated intensity and track of the tropical cyclones over the North Indian Ocean as well as improved the wind fields, temperature and moisture analyses and short-range forecasts during the southwest monsoon period (Deb et al., 2016; Kumar et al., 2016; Sharma et al., 2021).

In addition, following products are also generated which are derived from the wind products (Sankhala et al., 2021): (a) Relative vorticity at 850, 700, 500 and 200 hPa, (b) Wind shear, (c) Wind shear tendency, (d) Mid-level wind shear, (e) Lower convergence, and (f) Upper divergence.

Apart from the above mentioned geophysical products, several other products are also generated regularly from both INSAT-3D and INSAT-3DR VHRRs through MMDRPS. Some of these geophysical products are: (a) Cloud mask, (b) Cloud top temperature, (c) Cloud top pressure, (d) Cloud optical thickness, (e) Cloud particle effective radius, (f) Total precipitable water, (g) Storm Index, (h) Aerosol optical depth, (i) Fire, (j) Smoke, (k) Snow cover, (l) Snow depth, (m) Surface insolation, (n) Land surface albedo, (o) Net effective radiation, (p) Potential evapotranspiration, (q) Actual evapotranspiration, (r) Global horizontal irradiance, (s) Diffused normal irradiance, and (t) Direct horizontal irradiance. Some of these products are relevant to cloud microphysical and cloud properties (John et al., 2019; Lima et al., 2019, 2021; Gangwar and Thapliyal, 2022), whereas some are useful for hydro-meteorological and agro-meteorological applications (Shukla and Pal, 2009; Mishra, 2018; Pandya et al., 2021; Mishra et al., 2023). Cloud properties and cloud microphysical products have shown potential for extreme rainfall and thunderstorm nowcasting over the Indian region (Goyal et al., 2017b; Shukla et al., 2017). Furthermore, imager data products from INSAT-3D/3DR have shown to be vital for analyzing the spatiotemporal distributions of particulate matter concentration and for detection of dust storms over India and surrounding regions (Mishra et al., 2015;

Table 3. List of INSAT-3DR Sounder products operationally generated through the MMDRPS at IMD, New Delhi.

INSAT-3DR Sounder Products (For both sectors A & B)	
Band Images (18 images)	SWIR (1-6), MWIR (1-5), LWIR (1-7)
Band Temperature (18 images)	SWIR (1-6), MWIR (1-5), LWIR (1-7)
Geopotential Height Profiles (17 images)	1000, 950, 850, 700, 620, 500, 400, 300, 250, 200, 150, 100, 70, 50, 30, 20 & 10 hPa
Temperature Profiles (17 images)	1000, 950, 850, 700, 620, 500, 400, 300, 250, 200, 150, 100, 70, 50, 30, 20 & 10 hPa
Humidity Profiles (12 images)	1000, 950, 850, 700, 620, 500, 400, 300, 250, 200, 150 & 100 hPa
Products (13 images)	Dry Microburst Index, L1 Precipitable Water (1000-900 hPa), L2 Precipitable Water (900-700 hPa), L3 Precipitable Water (700-300 hPa), Total Precipitable Water Vapour, Total Ozone, Lifted Index, Wind Index, Cloud top pressure, Cloud top temperature, Effective cloud emissivity, Max vertical Theta-e, Surface skin temperature
T-Phi grams for clear sky pixels for about 730 stations	

Gupta et al., 2021; Sujitha et al., 2022). Recently, one new product namely, storm index has been developed using INSAT-3D/3DR OLR dataset for real-time thunderstorm monitoring over the Indian region (Mishra et al., 2023).

3.2 Data Products from INSAT-3D/3DR Sounder

The 19-channel sounder onboard the INSAT-3D satellite was the first atmospheric sounder on the INSAT series satellites which declared its end of life in September, 2020. Currently, sounder onboard the INSAT-3DR satellite is providing useful data at hourly interval. It provides hourly data 20 times a day for sector A (Indian land region) and 4 times a day for sector B (Indian Ocean region). The scan strategy of INSAT-3DR sounder was rescheduled after decommissioning of INSAT-3D sounder, and current scan mechanism of INSAT-3DR sounder is presented in Figure 4. Images of each band and their respective brightness temperatures are generated at hourly interval through the MMDRPS. In addition, profiles of geopotential height and temperature are operationally generated at 17 different pressure levels between 1000 hPa and 10 hPa. The humidity profiles are generated at 12 different pressure levels between 1000 hPa and 100 hPa. Following products and thermodynamic variables are also generated from the sounder data for clear-sky conditions: (a) Precipitable water between 1000 hPa and 900 hPa, (b) Precipitable water between 900 hPa and 700 hPa, (c) Precipitable water between 700 hPa and 300 hPa, (d) Total precipitable water vapour, (e) Total ozone, (f) Dry microburst index, (g) Lifted index, (h) Wind index, (i) Cloud top pressure, (j) Cloud top temperature, (k) Effective cloud emissivity, (l) Maximum vertical theta-e, and (m) Surface skin temperature. Furthermore, T-Phi grams for clear-sky pixels for about 730 stations across India are generated from the INSAT-3DR sounder data. A complete list of INSAT-3DR sounder imageries and products are provided in Table 3. Using 3D VAR data assimilation in a NWP model, larger impact of clear-sky sounder radiances than VHRR in short-range weather prediction was noticed (Singh et al., 2016a). In addition, WV sensitive channels of the sounder showed higher impact in short-range precipitation forecasts when compared to temperature-sensitive channels.

Vertical profiles and other derived indices from the INSAT-3DR sounder at about 10 km × 10 km spatial resolution are getting affected by the presence of clouds and surface properties. However, geophysical products for the clear-sky condition are proven to be very useful in weather forecasting and understanding the atmospheric dynamics (Jindal et al., 2014; Parihar et al., 2018;

Kumar and Ratnam, 2019; Prakash et al., 2022). Temperature profiles derived from the INSAT-3DR sounder have been evaluated over India against radiosonde measurements and positive bias of 1-3 K was reported (Giri et al., 2022). Similar positive bias in temperature profiles was also observed for the INSAT-3D sounder derived temperature profiles over India (Mitra et al., 2015; Ratnam et al., 2016; Singh et al., 2017). Total precipitable water product was compared with reanalysis product and validated against in-situ observations over the Indian sub-continent, and seasonal and regional variations in error characteristics were noted (Rao et al., 2020; Yadav et al., 2020, 2021). Total column ozone derived from the INSAT-3D sounder showed good agreement with the Atmospheric Infrared Sounder (AIRS) and ground-based observations over India, and proven to be useful in better understanding of its spatiotemporal variability across the country (Kumar et al., 2021). Lifted index, maximum vertical theta-e differential, wind index and dry microburst index are very useful for the detection of thunderstorm and convective activities. Lifted index, maximum vertical theta-e differential and dry microburst index are derived from the temperature and humidity profiles of the sounder. Wind index provides guidance on the maximum probable wind gusts, and is derived from the geopotential height, temperature and humidity profiles at standard pressure levels. Cloud-free temperature and WV products from the sounder were also used for the retrieval of convective available potential energy over the Indian region (Murali Krishna et al., 2019). Moreover, a preliminary validation of INSAT-3D and INSAT-3DR VHRR and sounder products was jointly carried out by IMD and SAC-ISRO, and an internal report was prepared in late 2021. Furthermore, IMD and SAC-ISRO jointly initiated the reprocessing of historical VHRR data of INSAT series meteorological satellites in order to generate a long-term climate data record (CDR) over the Indian region. This dataset will be useful for climate change studies and fill the gap in the global CDR.

References

Agarwal, N., R. Sharma, P. Thapliyal, R. Gangwar, P. Kumar, and R. Kumar, 2019: Geostationary satellite-based observations for ocean applications. Curr. Sci., 117, 506-515.

Agnihotri, C.L., 1993: Study of double ITCZ over Indian Ocean as revealed by INSAT cloud imagery and its role for southwest monsoon. Mausam, 44, 298-300.

Ahmed, R., S. Prakash, M. Mohapatra, R.K. Giri, and S. Dwivedi, 2022: Understanding the rapid intensification of extremely severe cyclonic storm ‘Tauktae’ using remote-sensing observations. Meteorol. Atmos. Phys., 134, 97.

Ahmed, R., M. Mohapatra, R.K. Giri, and S. Dwivedi, 2021: An evaluation of the Advanced Dvorak Technique (9.0) for the tropical cyclones over the North Indian Ocean. Trop. Cyclone Res. Rev., 10, 201-208.

Bhatia, R.C., and A.K. Mitra, 2021: 50 years of satellite meteorology in India. Vayumandal, 47, 47-58.

Bhatia, R.C., and A.K. Sharma, 2013: Recent advances in observational support from space-based systems for tropical cyclones. Mausam, 64, 97-104.

Bhatia, R.C., and H.V. Gupta, 1999: Use of charged coupled device payload on INSAT-2E for meteorological and agricultural applications. Curr. Sci., 76, 1444-1447.

Bhatia, R.C., B. Bhushan, and V.R. Rao, 1999: Applications of water-vapour imagery received from INSAT-2E satellite. Curr. Sci., 76, 1448-1450.

Bhattacharya, B.K., N. Padmanabhan, M. Sazid, R. Ramakishna, and J.S. Parihar, 2013: Assessment of potential solar energy over India using diurnal remote sensing observations using Indian geostationary satellite data. Int. J. Remote Sens., 34, 7069-7090.

Bushair, M.T., P. Kumar, and R.M. Gairola, 2019: Evaluation and assimilation of various satellite-derived rainfall products over India. Int. J. Remote Sens., 40, 5315-5338.

Chattopadhyay, N., S.S. Vyas, B.K. Bhattacharya, and S. Chandras, 2016: Evaluating the potential of rainfall product from Indian geostationary satellite

for operational agromet advisory services in India. J. Agrometeorol., 18, 29-33.

Chaurasia, S., and R.K. Jenamani, 2017: Detection of fog using temporally consistent algorithm with INSAT-3D imager data over India. IEEE J. Selected Topics Earth Obs. Remote Sens., 10, 5307-5313.

Chaurasia, S., and B.S. Gohil, 2015: Detection of day time fog over India using INSAT-3D data. IEEE J. Selected Topics Earth Obs. Remote Sens., 8, 4524-4530.

Deb, S.K., D.K. Sankhala, P. Kumar, and C.M. Kishtawal, 2020: Retrieval and applications of atmospheric motion vectors derived from Indian geostationary satellites INSAT-3D/INSAT-3DR. Theor. Appl. Climatol., 140, 751-765.

Deb, S.K., D.K. Sankhala, and C.M. Kishtawal, 2018: Retrieval of atmospheric motion vector using INSAT-3D and INSAT-3DR imager data in staggering mode. Vayumandal, 42, 31-46.

Deb, S.K., C.M. Kishtawal, P. Kumar, A.S. Kiran Kumar, P.K. Pal, N. Kaushik, and G. Sangar, 2016: Atmospheric motion vectors from INSAT-3D: initial quality assessment and its impact on track forecast of cyclonic storm Nanauk. Atmos. Res., 169, 1-16.

Dvorak, V.F., 1975: Tropical cyclone intensity analysis and forecasting from satellite imagery. Mon. Wea. Rev., 103, 420-430.

Gairola, R.M., S. Prakash, M.T. Bushair, and P.K. Pal, 2014: Rainfall estimation from Kalpana-1 satellite data over Indian land and oceanic regions. Curr. Sci., 107, 1275-1282.

Gangwar, R.K., and P.K. Thapliyal, 2022: Optimal estimation of total precipitable water from INSAT-3D/3DR imagers. Quart. J. Royal Meteorol. Soc., 148, 466-479.

Gangwar, R.K., and P.K. Thapliyal, 2020: Variational based estimation of sea surface temperature from split-window observations of INSAT-3D/3DR imager. Remote Sens., 12, 3142.

Ghanekar, S.P., P.V. Puranik, and V.R. Mujumdar, 2010: Application of satellite-derived OLR data in the prediction of the onset of Indian summer monsoon. Theor. Appl. Climatol., 99, 457-468.

Giri, R.K., R. Yadav, M. Ranalkar, and V. Singh, 2022: Validation of INSAT-3DR sounder retrieved temperature profile with GPS radiosonde and AIRS observations. Adv. Space Res., 69, 1100-1115.

Goyal, S., M. Mohapatra, P. Kumari, S.K. Dube, and K. Rajendra, 2017a: Validation of Advanced Dvorak Technique (ADT) over north Indian Ocean. Mausam, 68, 689-698.

Goyal, S., A. Kumar, M. Mohapatra, L.S. Rathore, S.K. Dube, R. Saxena, and R.K. Giri, 2017b: Satellite-based technique for nowcasting of thunderstorms over Indian region. J. Earth Syst. Sci., 126, 79.

Gupta, A., Y. Kant, D. Mitra, and P. Chauhan, 2021: Spatio-temporal distribution of INSAT-3D AOD derived particulate matter concentration over India. Atmos. Poll. Res., 12, 159-172.

Jaiswal, N., S.K. Deb, and C.M. Kishtawal, 2022: Intensification of tropical cyclone FANI observed by INSAT-3DR rapid scan data. Theor. Appl. Climatol., 148, 661-670.

Jangid, B.P., S. Prakash, M.T. Bushair, and R. Kumar, 2017: Adding value to INSAT-3D sea surface temperature fields using MODIS data over the tropical Indian Ocean. Remote Sens. Lett., 8, 458-467.

Jindal, P., P.K. Thapliyal, M.V. Shukla, A.K. Mishra, and D. Mitra, 2014: Total column ozone retrieval using INSAT-3D sounder in the tropics: a simulation study. J. Earth Syst. Sci., 123, 1265-1271.

John, J., I. Dey, A. Pushpakar, V. Sathiyamoorthy, and B.P. Shukla, 2019: INSAT-3D cloud microphysical product: retrieval and validation. Int. J. Remote Sens., 40, 1481-1494.

Joseph, G., V.S. Iyengar, K. Nagachechaiah, A.S. Kiran Kumar, B.V. Aradhye, V.N. Kaduskar, R.K. Dave, and C.M. Nagrani, 1994: Very high

resolution radiometers for INSAT-2. Curr. Sci., 66, 42-56.

Joshi, P.C., M.S. Narayanan, R.C. Bhatia, B. Manikiam, A.S. Kiran Kumar, and V. Jayaraman, 2003: Evolution of Indian satellite meteorological programme. Mausam, 54, 1-12.

Kaila, V.K., A.S. Kiran Kumar, T.K. Sundaramurthy, S. Ramakrishnan, M.Y.S. Prasad, P.S. Desai, V. Jayaraman, and B. Manikiam, 2002: METSAT - a unique mission for weather and climate. Curr. Sci., 83, 1081-1088.

Katti, V.K., V.R. Pratap, R.K. Dave, and K.N. Mankad, 2006: INSAT-3D: an advanced meteorological mission over Indian Ocean. Proc. SPIE 6407, GEOSS and Next-Generation Sensors and Missions, 640709.

Kelkar, R.R., 2019: Satellite meteorology in India: its beginning, growth and future. Mausam, 70, 1-14.

Kelkar, R.R., H.V. Gupta, and L.R. Meena, 1992: Use of INSAT for observation and communication of meteorological information. IETE Tech. Rev., 9, 214-221.

Kelkar, R.R., and A.V.R.K. Rao, 1990: Interannual variability of monsoon rainfall as estimated from INSAT-1B data. Mausam, 41, 183-188.

Kishtawal, C.M., 2016: Use of satellite observations in tropical cyclone studies. In Advanced Numerical Modeling and Data Assimilation Techniques for Tropical Cyclone Prediction Mohanty U.C., Gopalakrishnan S.G. (eds). 35-47, Springer, Dordrecht.

Kishtawal, C.M., 2019: Use of satellite observations for weather prediction. Mausam, 70, 709-724.

Khan, A.W., C. Mahesh, M.T. Bushair, and R.M. Gairola, 2021: Estimation and evaluation of rainfall from INSAT-3D improved IMSRA algorithm during 2018 summer monsoon season. J. Earth Syst. Sci., 130, 37.

Konduru, R.T., C.M. Kishtawal, and S. Shah, 2013: A new perspective on the infrared brightness temperature distribution of the deep convective clouds. J. Earth Syst. Sci., 122, 1195-1206.

Kumar, A.H., and M.V. Ratnam, 2019: Tropical tropopause layer characteristics observed at different scales over the complete Indian region using INSAT-3D sounder measurements. Curr. Sci., 117, 1813-1827.

Kumar, A., A.K. Singh, J.N. Tripathi, M. Sateesh, and V. Singh, 2021: Evaluation of INSAT-3D-derived Hydro-Estimator and INSAT Multi-Spectral Rain Algorithm over tropical cyclones. J. Indian Soc. Remote Sens., 49, 1633-1650.

Kumar, P., M.V. Shukla, and A.K. Varma, 2022: Impact of all-sky water vapour channel radiance from INSAT-3D/3DR satellite over South Asia region using WRF model. Quart. J. Royal Meteorol. Soc., 148, 2532-2545.

Kumar, P., and A.K. Varma, 2017: Assimilation of INSAT-3D hydro-estimator method retrieved rainfall for short-range weather prediction. Quart. J. Royal Meteorol. Soc., 143, 384-394.

Kumar, P., S.K. Deb, C.M. Kishtawal, and P.K. Pal, 2016: Impact of assimilation of INSAT-3D retrieved atmospheric motion vectors on short-range forecast of summer monsoon 2014 over the South Asian region. Theor. Appl. Climatol., 128, 575-586.

Kumar, R.R., K.R. Vankayalapati, V.K. Soni, H.P. Dasari, M.K. Jain, A. Tiwari, R.K. Giri, and S. Desamsetti, 2021: Comparison of INSAT-3D retrieved total column ozone with ground-based and AIRS observations over India. Sci. Total Environ., 793, 148518.

Lima, C.B., S.S. Prijith, P.V.N. Rao, M.V.R.S. Sai, and M.V. Ramana, 2021: Quality estimates of INSAT-3D derived cloud top temperature for climate data record. IEEE Trans. Geosci. Remote Sens., 59, 5417-5422.

Lima, C.B., S.S. Prijith, M.V.R. Sesha Sai, P.V.N. Rao, K. Niranjan, and M.V. Ramana, 2019: Retrieval and validation of cloud top temperature from the geostationary satellite INSAT-3D. Remote Sens., 11, 2811.

Lodh, A., G. George, H. Singh, J.P. George, and E.N. Rajagopal, 2019: Assimilation of INSAT-3D land surface temperature in EKF based land data

assimilation system. NCMRWF Technical Report, 19 pp., NMRF/TR/07/2019.

Mahesh, C., S. Prakash, V. Sathiyamoorthy, and R.M. Gairola, 2014: An improved approach for rainfall estimation over Indian summer monsoon region using Kalpana-1 data. Adv. Space Res., 54, 685-693.

Malhan, T., N. Sehgal, R.K. Giri, C. Mishra, L. Pathak, R. Sharma, and S. Kumar, 2022: Comparative analysis of sub division wise rainfall INSAT-3D vs ground based observations. Mausam, 73, 833-842.

Manikiam, B., and K. Nagaraja, 2015: Satellite based climate change study. Vayumandal, 41, 53-61.

Mathur, A., I. Srinivasan, B.S. Gohil, A. Sarkar, and V.K. Agarwal, 2006: Development of sea surface temperature retrieval algorithm for INSAT-3D. Proceedings Vol. 6404, Remote Sensing and Modeling of the Atmosphere, Oceans, and Interactions, SPIE Asia-Pacific Remote Sensing.

Mishra, A.K., A.K. Mitra, and S.C. Bhan, 2023: Towards development of storm index using satellite observation for near real-time monitoring of thunderstorm over India. Weather, 78, 113-116.

Mishra, M.K., 2018: Retrieval of aerosol optical depth from INSAT-3D imager over Asian landmass and adjoining ocean: retrieval uncertainty and validation. J. Geophys. Res. - Atmos., 123, 5484-5508.

Mishra, M.K., P. Chauhan, and A. Sahay, 2015: Detection of Asian dust storms from geostationary satellite observations of the INSAT-3D imager. Int. J. Remote Sens., 36, 4668-4682.

Mitra, A.K., S. Parihar, S.K. Peshin, R. Bhatla, and R.S. Singh, 2019: Monitoring of severe weather events using RGB scheme of INSAT-3D satellite. J. Earth Syst. Sci., 128, 36.

Mitra, A.K., S. Parihar, R. Bhatla, and K.J. Ramesh, 2018a: Identification of weather events from INSAT-3D RGB scheme using RAPID tool. Curr. Sci., 115, 1358-1366.

Mitra, A.K., N. Kaushik, A.K. Singh, S. Parihar, and S.C. Bhan, 2018b: Evaluation of INSAT-3D satellite derived precipitation estimates for heavy rainfall events and its validation with gridded GPM (IMERG) rainfall dataset over the Indian region. Remote Sens. Appl.: Soc. Environ., 9, 91-99.

Mitra, A.K., S.C. Bhan, A.K. Sharma, N. Kaushik, S. Parihar, R. Mahandru, and P.K. Kundu, 2015: INSAT-3D vertical profile retrievals at IMDPS, New Delhi: a preliminary evaluation. Mausam, 66, 687-694.

Mohapatra, M., A.K. Mitra, V. Singh, S.K. Mukherjee, K. Navria, V. Prashar, A. Tyagi, A.K. Verma, S. Devi, V.S. Prasad, M. Ramesh, and R. Kumar, 2021: INSAT-3DR-rapid scan operations for weather monitoring over India. Curr. Sci., 120, 1026-1034.

Murali Krishna, U.V., S.K. Das, K.N. Uma, and G. Pandithurai, 2019: Retrieval of convective available potential energy from INSAT-3D measurements: comparison with radiosonde data and their spatial-temporal variations. Atmos. Meas. Tech., 12, 777-790.

Nadimpalli, R., A. Srivastava, V.S. Prasad, K.K. Osuri, A.K. Das, U.C. Mohanty, and D. Niyogi, 2020: Impact of INSAT-3D/3DR radiance data assimilation in predicting tropical cyclone Titli over the Bay of Bengal. IEEE Trans. Geosci. Remote Sens., 58, 6945-6957.

Nayak, S., 2020: Remote sensing for national development: the legacy of Dr. Vikram Sarabhai. J. Indian Soc. Remote Sens., 48, 1101-1120.

Ojha, S.P., and R. Singh, 2019: Physical retrieval of sea-surface temperature from INSAT-3D imager observations. Tellus A: Dyn. Meteorol. Ocean., 71, 1554421.

Pal, P.K., B.M. Rao, C.M. Kishtawal, M.S. Narayanan, and G. Rajkumar, 1989: Cyclone track prediction using INSAT data. Proc. Indian Acad. Sci. (Earth Planet Sci.), 98, 353-364.

Pandya, M.R., V. Pathak, N. Kaushik, and H.J. Trivedi, 2021: Algorithm for the estimation of continental scale land-surface broadband albedo

from INSAT-3D imager data. J. Indian Soc. Remote Sens., 49, 2093-2102.

Pandya M.R., D.B. Shah, H.J. Trivedi, S. Panigrahy, and J.S. Parihar, 2011: Evaluation of split-window algorithms for retrieving land surface temperature from the INSAT-3D imager observations. Vayumandal, 37, 31-37.

Parihar, S., A.K. Mitra, M. Mohapatra, and R. Bhatla, 2018: Potential of INSAT-3D sounder-derived total precipitable water product for weather forecast. Atmos. Meas. Tech., 11, 6003-6012.

Patel, S., S. Prakash, and B. Bhatt, 2015: An assessment of Kalpana-1 rainfall product for drought monitoring over India at meteorological sub-division scale. Water Int., 40, 689-702 .

Prakash, S., A. Kumar, R. Sharma, S. Kumar, and R.K. Giri, 2022: INSAT-3D/3DR and GNSS derived products and thunderstorm events over the India region. J. Sci. Technol. Res., 4, 44-50.

Prakash, S., and S.C. Bhan, 2023b: How accurate are infrared-only and rain gauge-adjusted multi-satellite precipitation products in the southwest monsoon precipitation estimation across India?, Environ. Monitor. Assess., 195, 515.

Prakash, S., and S.C. Bhan, 2023a: Assessment of INSAT-3D-derived high-resolution real-time precipitation products for North Indian Ocean cyclones. Nat. Haz., 115, 993-1009.

Prakash, S., C. Mahesh, and R.M. Gairola, 2011: Large-scale precipitation estimation using Kalpana-1 IR measurements and its validation using GPCP and GPCC data. Theor. Appl. Climatol., 106, 283-293.

Prakash, S., C. Mahesh, R.M. Gairola, and P.K. Pal, 2010: Estimation of Indian summer monsoon rainfall using Kalpana-1 VHRR data and its validation using rain gauge and GPCP data. Meteorol. Atmos. Phys., 110, 45-57.

Rani, S.I., R. Taylor, P. Sharma, M.T. Bushair, B.P. Jangid, J.P. George, and E.N. Rajagopal, 2019: Assimilation of INSAT-3D imager water vapour clear sky brightness temperature in the NCMRWF's assimilation and forecast system. J. Earth Syst. Sci., 128, 197.

Rao, V.K., A.K. Mitra, K.K. Singh, G. Bharathi, R.R. Kumar, K. Ray, and S.S.V.S. Ramakrishna, 2020: Evaluation of INSAT-3D derived TPW with AIRS retrievals and GNSS observations over the Indian region. Int. J. Remote Sens., 41, 1139-1169.

Ratnam, M.V., A.H. Kumar, and A. Jayaraman, 2016: Validation of INSAT-3D sounder data with in situ measurements and other similar satellite observations over India. Atmos. Meas. Tech., 9, 5735-5745.

SAC, 2015: INSAT-3D algorithm theoretical basis development document. Space Applications Centre, ISRO, Ahmedabad, India, pp. 379. Available at https://mosdac.gov.in/data/doc/INSAT_3D_ATBD_MAY_2015.pdf

Sankhala, D.K., S.K. Deb, and N. Jaiswal, 2021: Wind derived products using INSAT-3D atmospheric motion vectors and its meteorological applications. Int. J. Remote Sens., 42, 1357-1378.

Sankhala, D.K., S.K. Deb, and V. Sathiyamoorthy, 2019: INSAT-3D low-level atmospheric motion vectors: capability to capture Indian summer monsoon intra-seasonal variability. J. Earth Syst. Sci., 128, 31.

Sharma, P., S.I. Rani, and M. Das Gupta, 2021: Validation and assimilation of INSAT atmospheric motion vectors: case studies for tropical cyclones. J. Earth Syst. Sci., 130, 235.

Shukla, B.P., C.M. Kishtawal, and P.K. Pal, 2017: Satellite-based nowcasting of extreme rainfall events over western Himalayan region. IEEE J. Selected Topics Appl. Earth Obs. Remote Sens., 10, 1681-1686.

Shukla, B.P., and P.K. Pal, 2009: Automatic smoke detection using satellite imagery: preparatory to smoke detection from INSAT-3D. Int. J. Remote Sens., 30, 9-22.

Singh, A. K., V. Singh, K. K. Singh, J. N. Tripathi, A. Kumar, M. Sateesh, and S. K. Peshin, 2018: Validation of INSAT-3D derived rainfall estimates (HE & IMSRA), GPM (IMERG) and GLDAS 2.1

model rainfall product with IMD gridded rainfall & NMSG data over IMD's meteorological sub-divisions during monsoon. Mausam, 69, 177-192.

Singh, D., R.C. Bhatia, S.K. Srivasatav, S. Prasad, and R.K. Giri, 2006: Operational use of improved CMVs derived from INSAT IR data in NWP model over Indian region. Mausam, 57, 315-322.

Singh, J., R.K. Giri, and S. Kant, 2007: Radiation fog viewed by INSAT-1D and Kalpana geo-stationary satellite. Mausam, 58, 251-260.

Singh, R., C. Singh, S.P. Ojha, A. S. Kumar, C.M. Kishtawal, and A.S.K. Kumar, 2016b: Land surface temperature from INSAT-3D imager data: retrieval and assimilation in NWP model. J. Geophys. Res. - Atmos., 121, 6909-6926.

Singh, R., S.P. Ojha, C.M. Kishtawal, P.K. Pal, and A.S. Kiran Kumar, 2016a: Impact of the assimilation of INSAT-3D radiances on short-range weather forecasts. Quart. J. Royal Meteorol. Soc., 142, 120-131.

Singh, R., P.K. Thapliyal, C.M. Kishtawal, P.K. Pal, and P.C. Joshi, 2007: A new technique for estimating outgoing longwave radiation using infrared window and water vapor radiances from Kalpana very high resolution radiometer. Geophys. Res. Lett., 34, L23815.

Singh, T., R. Mittal, and M.V. Shukla, 2017: Validation of INSAT-3D temperature and moisture sounding retrievals using matched radiosonde measurements. Int. J. Remote Sens., 38, 3333-3355.

Srinivasan, J.S., and P.C. Joshi, 2007: What have we learned about the Indian monsoon from satellite data?, Curr. Sci., 93, 165-172.

Sujitha, P.R., P. Santra, A.K. Bera, M.K. Verma, and S.S. Rao, 2022: Detecting dust loads in the atmosphere over Thar desert by using MODIS and INSAT-3D data. Aeolian Res., 57, 100814.

Thapliyal, P.K., M.V. Shukla, S. Sah, P.C. Joshi, P.K. Pal, and K.S. Ajil, 2011: An algorithm for the estimation of upper tropospheric humidity from Kalpana observations: methodology and validation. J. Atmos. Res. - Atmos., 116, D01108.

Varma, A.K., and N. Sharma, 2022: Modified Hydro-Estimator: pixel-scale instantaneous measurement of precipitation from Indian geostationary satellites. J. Indian Soc. Remote Sens., 50, 2163-2173.

Veeraraghavan, K., and V.S. Tiwari, 1984: Tracking of a cyclone over Arabian Sea by enhanced satellite pictures. Mausam, 35, 67-70.

Velden, C., et al., 2006: The Dvorak tropical cyclone intensity estimation technique - a satellite-based method that has endured for over 30 years. Bull. Amer. Meteorol. Soc., 87, 1195-1210.

Vyas, S.S., and B.K. Bhattacharya, 2020: Agricultural drought early warning from geostationary meteorological satellites: concept and demonstration over semi-arid tract in India. Environ. Monit. Assess., 192, 311.

Vyas, S.S., B. K. Bhattacharya, R. Nigam, P. Guhathakurta, K. Ghosh, N. Chattopadhyay, and R. M. Gairola, 2015: A combined deficit index for regional agricultural drought assessment over semi-arid tract of India using geostationary meteorological satellite data. Int. J. Appl. Earth Obs. Geoinf., 39, 28-39.

Yadav, R., R.K. Giri, and S.C. Bhan, 2022: High-resolution outgoing long wave radiation data (2014-2020) of INSAT-3D imager and its comparison with Clouds and Earth's Radiant Energy System (CERES) data. Adv. Space Res., 70, 976-991.

Yadav, R., R.K. Giri, and V. Singh, 2021: Intercomparison review of IPWV retrieved from INSAT-3DR sounder, GNSS and CAMS reanalysis data. Atmos. Meas. Tech., 14, 4857-4877.

Yadav, R., N. Puviarasan, R.K. Giri, C.S. Tomar, and V. Singh, 2020: Comparison of GNSS and INSAT-3D sounder retrieved precipitable water vapour and validation with the GPS sonde data over Indian subcontinent. Mausam, 71, 1-10.